Journal of Alloys and Compounds 726 (2017) 209–213

Contents lists available at ScienceDirect

Journal of Alloys and Compounds

journal homepage: http://www.elsevier.com/locate/jalcom

Investigation of energy transfer mechanism in Er^{3+} and Tm^{3+} doped AlN crystalline films

X.D. Wang [a, **, 1], M.M. Yang [b, 1], X.H. Zeng [b, *], Y.J. Mo [a], J.C. Zhang [b], J.F. Wang [b], K. Xu [b, ***]

[a] *Jiangsu Key Laboratory of Micro and Nano Heat Fluid Flow Technology and Energy Application, School of Mathematics and Physics, Suzhou University of Science and Technology, Suzhou, Jiangsu 215009, PR China*
[b] *Suzhou Institute of Nano-tech and Nano-bionics, Chinese Academy of Sciences, Suzhou, Jiangsu 215123, PR China*

ARTICLE INFO

Article history:
Received 30 March 2017
Received in revised form
26 July 2017
Accepted 31 July 2017
Available online 3 August 2017

Keywords:
AlN
Rare earth
Luminescence

ABSTRACT

In this work, Er-implanted AlN, Tm-implanted AlN and Er, Tm co-implanted AlN were prepared. All samples were annealed after ion-implantation. The optical and structural properties of the samples were characterized by cathodoluminescence and X-ray diffraction, respectively. For Er-implanted AlN, the dominant sharp emission lines centered at 410 and 480 nm were observed. For Tm-implanted AlN, the dominant sharp emission line centered at 467 nm was observed. After Er was implanted into AlN: Tm, the intensity ratio of 370 nm and 467 nm in Er, Tm co-implanted AlN is almost 10 times of that in AlN: Tm. Meanwhile, the Tm emission lines centered at 685 nm and 776 nm disappeared, which can be illuminated on the viewpoint of near resonance energy transfer between Tm and Er in AlN host.

1. Introduction

Rare earth (RE) ions activated aluminum nitride (AlN) films are promising for developing new photoelectric devices and optical amplifiers. Due to shielded 4f inner shell electrons, the intra 4f-4f transitions of rare earth ions are insensitive to the host, and the emission spectra cover the wavelength range from ultraviolet (UV) to infrared (IR). Compared with other semiconductors, such as Si and GaN, AlN has wider band gap, therefore, weaker thermal quenching of rare earth luminescence in AlN is expected [1–3]. In recent years, N. Nepal et al. reported a remarkable emission peak centered at 298 nm has been detected in Tm doped AlN thin films grown by molecular beam epitaxy [4]. Muhammad Maqboola et al. prepared the Er doped amorphous AlN films by radio-frequency sputtering and observed green luminescence peaks centered at 538 nm and 560 nm [5].

When two or more kinds of RE ions were co-doped into AlN host together, energy transfer (ET) process maybe available due to abundant energy levels of RE ions. Generally, the ET process between RE ions can be realized through resonance energy transfer mechanism due to the near-field force between RE ions. Based on the up conversion mechanism, white light emitting was achieved in RE ions co-doped transparent ceramics [6–8]. Muhammad Maqboola et al. reported the energy transfer mechanism between Er^{3+} and Yb^{3+} in Er, Yb co-doped amorphous AlN films grown by radio-frequency magnetron sputtering [9]. However, different from the ceramic or amorphous AlN, RE ions mainly occupy the Al lattice sites in crystalline AlN films [10–12]. The different lattice symmetry may generate the different luminescence feature. Besides, the luminescence of Er^{3+} and Tm^{3+} co-doped AlN crystalline materials have not been reported up till now. In this work, we prepared Er^{3+} and Tm^{3+} co-implanted *c*-axis oriented crystalline AlN films and thermal annealing was used to remove the damage induced by ion implantation. The energy transfer mechanism in Er^{3+} and Tm^{3+} co-implanted AlN crystalline films was investigated in detail.

2. Experimental details

AlN films with 2 μm thickness were grown on sapphire substrate by hydride vapor phase epitaxy (HVPE) and the growth details were reported elsewhere [13]. Er-implanted AlN, Tm-implanted AlN and Er, Tm co-implanted AlN were prepared respectively. In all samples, the dose of Er is 1×10^{15} at/cm^2 and the dose of Tm is 1×10^{15} at/cm^2. In ion-implantation process AlN films was kept at room temperature, the implantation energy is 200 keV,

---

* Corresponding author.
** Corresponding author.
*** Corresponding author.
E-mail addresses: xdwang0416@163.com (X.D. Wang), xhzeng2007@sinano.ac.cn (X.H. Zeng), kxu2006@sinano.ac.cn (K. Xu).
[1] X.D. Wang and M. M. Yang contribute equally to this work.

http://dx.doi.org/10.1016/j.jallcom.2017.07.334
0925-8388/© 2017 Elsevier B.V. All rights reserved.

and the implanting ion beam was inclined about 10° with respect to the normal of (0002) plane of the AlN films for reducing the channeling effect. All implanted samples were successively annealed at 1050 °C for 1 h and 1100 °C for 1 h under a flow of N_2 at one atmospheric pressure. The structure evolution of implanted samples before and after annealing was characterized by high resolution X-ray diffraction (HRXRD). Luminescence properties were measured by a MonoCL3+ cathodoluminescence spectrometer installed on a Quanta400FEG field emission scanning electron microscope (SEM). All measurements were carried out at room temperature.

3. Results and discussion

Fig. 1(a) is the θ-2θ curve of Er, Tm co-implanted AlN. The diffraction peaks at 34.5°, 72.8° are corresponding to (0002) and (0004) plane of AlN, respectively. The diffraction peak at 41.7° is corresponding to (0006) plane of the sapphire substrate. No other phase was detected within the sensitivity of XRD measurements. Fig. 1(b) shows the (0002) peak of θ-2θ curves of as-grown AlN, Er, Tm co-implanted AlN and 1050 °C annealed Er, Tm co-implanted AlN. After Er and Tm implantation, several satellite peaks at lower angle were observed on the left side of AlN (0002) reflection, indicating the increment of the lattice parameters along the c-axis. Previous studies have indicated that the ion implantation process would generate a mass of stacking faults and clusters of point defects, especially in the worst damage area [14,15]. Within the ions implantation process, the interaction between point defects and stacking faults in damage area was enhanced increasingly, which may result in more than one satellite peaks. After 1050 °C annealing, a satellite peak still was observed, which indicates that the damage caused by ion implantation could not be removed completely.

The CL spectrum of AlN: Er^{3+} annealed at 1050 °C was shown in Fig. 2(a). A clear broad peak at 378 nm is belong to the oxygen impurity which is located on substitutional N site and form a defect complex with Al vacancy, namely O_N-V_{Al} [16–18]. Two obvious emission peaks at 410 nm and 480 nm were belong to transitions from the excited state $^2H_{9/2}$ and $^4F_{7/2}$ to the ground state $^4I_{15/2}$, respectively, which is different from the Er-doped GaN [19] and Er-doped amorphous AlN [20]. Much weaker emission peaks between 500 nm and 900 nm is originated from the transitions of $^4H_{11/2} \rightarrow {}^4I_{15/2}$ (537 nm), $^4S_{3/2} \rightarrow {}^4I_{15/2}$ (560 nm), $^2P_{3/2} \rightarrow {}^4S_{3/2}$ (771 nm) and $^4I_{9/2} \rightarrow {}^4I_{15/2}$ (819 nm). Especially, a broad band below 480 nm peak was observed. However, when the temperature was increased to 1100 °C, the broad band disappeared (See the inset of Fig. 2(a)), which indicates that the broad band maybe related to the defects induced by ion implantation. The results of positron annihilation have proved that the maximum concentration of cationic vacancy was produced in the worst damaged region during the ions implantation process [21]. Meanwhile the Al vacancy, acting as a deep acceptor level, is about 2.6 eV above the valence band [22]. Therefore, the broad band below 480 nm peak may be originated from the Al vacancy.

Fig. 2(b) was the CL spectrum of AlN:Tm^{3+} annealed at 1050 °C. Dominant CL emission peak has been observed at 467 nm which is assigned to $^1D_2 \rightarrow {}^3F_4$ transition. The other $^1D_2$-related emissions peaks at 370 nm, 684 nm, 527 nm and 776 nm are attributed to $^1D_2 \rightarrow {}^3H_6$, $^1D_2 \rightarrow {}^3H_4$,

$^1D_2 \rightarrow {}^3H_5$ and $^1D_2 \rightarrow {}^3F_3$ transitions, respectively. It was noted that $^1I_6$-related peaks also were observed in the spectrum: $^1I_6 \rightarrow {}^3H_6$ (297 nm), $^1I_6 \rightarrow {}^3F_4$ (357 nm) and $^1I_6 \rightarrow {}^3H_5$ (394 nm). Minor peaks were observed at 480 nm and 807 nm attributed to $^1G_4 \rightarrow {}^3H_6$ and $^3H_4 \rightarrow {}^3H_6$, respectively. Peaks at 597 nm, 714 nm and 741 nm (exactly double of 297 nm, 357 nm and 370 nm, respectively) were due to the second-order diffraction of spectrometer grating. The O_N-V_{Al} peak at 378 nm and the V_{Al} broad band below 480 nm peak as shown in Fig. 1(a) were not observed in Fig. 2(b), which may be due to the energy transfer process between Tm^{3+} and these defects. A possible resonance energy transfer mechanism was shown in Fig. 2(c). The energy gap of O_N to O_N-V_{Al} and V_{Al} to valence band is nearly equal to the energy gap of $^1D_2$ to $^3H_6$ and $^1G_4$ to $^3H_6$,

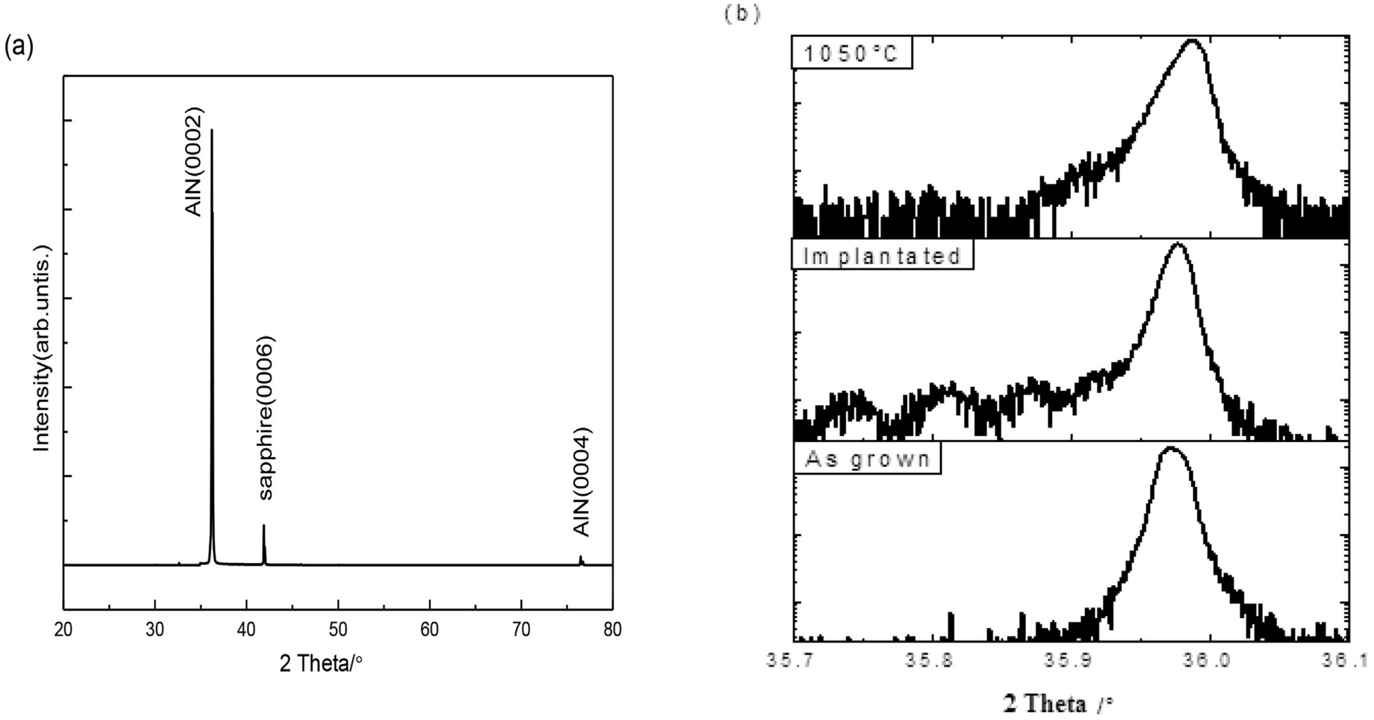

Fig. 1. (a) θ-2θ curve for Er and Tm co-implanted AlN; (b) (0002) peak of θ-2θ curves of as-grown AlN, Er and Tm co-implanted AlN and 1050 °C annealed Er, Tm co-implanted AlN.